

Politecnico di Milano

SCHOOL OF INDUSTRIAL AND INFORMATION ENGINEERING

Master of Science – Aerospace Engineering



Thesis Title

Supervisor

Title Name SURMANE

Co-Supervisor

Title Name SURNAME

Candidate

Claudio CACCIA – 820091

Academic Year 2019 – 2020

Acknowledgements

Thanks

Abstract

This thesis describes bla bla...

Keywords— one, two, three, four

Sommario

In questa tesi bla bla...

Contents

Acknowledgements	iii
Abstract	v
Sommario	vii
Contents	x
List of Figures	xi
List of Tables	xiii
1 Introduction	1
2 Physical aspects of Fluid-Structure Interaction problems	3
2.1 Description of motion	3
2.1.1 Eulerian perspective	3
2.1.2 Lagrangian perspective	4
2.1.3 ALE method	5
2.2 Domains and interface	6
2.2.1 Fluid domain	6
2.2.2 Solid domain	7
2.2.3 Models with reduced dimensionality: beams	8
2.2.4 Interface and interaction	9
2.3 Classification of FSI problems	10
2.3.1 Dimensional analysis	10
2.3.2 Dimensional analysis in fluid domain	11
2.3.3 Dimensional analysis in solid domain	12
2.3.4 Dimensional analysis of coupled problems	12
3 Computational aspects of Fluid-Structure Interaction problems	15
3.1 Monolithic and Partitioned Approach	15
3.2 Coupling Strategies	17
3.2.1 Explicit coupling schemes	17
3.2.2 Implicit coupling schemes	18
3.3 Strong coupling algorithms	20
3.3.1 under-relaxation	20
3.3.2 Quasi Newton Least Squares schemes	21
3.3.3 Convergence criteria	22
3.4 Interface Mesh and Data Mapping	23
3.4.1 Non-conforming Mesh methods	23

3.4.2	Conforming Mesh methods	24
3.4.3	Data Mapping	24
3.5	Stability: Added Mass Effect	25
4	Software Packages used in this work	29
4.1	preCICE	29
5	MBDyn Adapter and its integration	31
6	Validation Test-cases	33
7	Conclusions	35
	Conclusions	35
A	First Appendix	39
	Acronyms	45
	Bibliography	50

List of Figures

Figure 2.1	Eulerian perspective	4
Figure 2.2	Lagrangian perspective	4
Figure 2.3	ALE perspective	5
Figure 2.4	ALE mesh	6
Figure 2.5	beam model, taken from [1]	9
Figure 2.6	fluid solid interface	9
Figure 3.1	monolithic approach: S_f, S_s denote the fluid and the structure solutions	16
Figure 3.2	partitioned approach: S_f, S_s denote the fluid and the structure solutions, while σ and \vec{v} represent coupling data	16
Figure 3.3	Explicit coupling schemes	18
Figure 3.4	Implicit coupling schemes	19
Figure 3.5	non conforming mesh example	23
Figure 3.6	conforming mesh example	24
Figure 3.7	Examples of mapping data between non-coincident meshes: consistent (a) and conservative (b) schemes.	25

List of Tables

Table 2.1	fluid matrix of dimension exponents	11
-----------	---	----

Chapter 1

Introduction

Fluid-Structure Interaction (FSI) describes the mutual interaction between a moving or deformable object and a fluid in contact with it, surrounding or internal. It is present in various forms both in nature and in man-made systems: a leaf fluttering in the wind, water flowing underground or blood pumping in an artery are typical examples of fluid-structure interaction in nature. FSI occurs in engineered systems when modeling the behavior of turbomachinery, the flight characteristics of an aircraft, or the interaction of a building with the wind, just to name a few examples.

All the aforementioned problems go under the same category of FSI, even if the nature of the interaction between the solid and fluid is different. Specifically, the intensity of the exchanged quantities and the effect in the fluid and solid domains vary among different problems.

There can be multiple ways to classify FSI problems, based on the flow physics and on the behavior of the body. Incompressible flow assumption is always made for liquid-solid interaction, while both compressible and incompressible flow assumptions are made when a gas interacts with a solid, depending on the flow properties and the kind of simulation. The main application of air-solid interaction considers the determination of aerodynamic forces on structures such as aircraft wings, which is often referred to as *aeroelasticity*. Dynamic aeroelasticity is the topic that normally investigates the interaction between aerodynamic, elastic and inertial forces. Aerodynamic *flutter* (i.e. the dynamic instability of an elastic structure in a fluid flow) is one of the severe consequences of aerodynamic forces. It is responsible for destructive effects in structures and a significant example of FSI problem.

The subject may also be classified considering the behavior of the structure interacting with the fluid: a solid can be assumed rigid or deforming because of the fluid forces. Examples where rigid body assumption may be used include internal combustion engines, turbines, ships and offshore platforms. The rigid body–fluid interaction problem is simpler to some extent, nevertheless the dynamics of rigid body motion requires a solution that reflects the fluid forces. Within the deformable body–fluid interaction, the nature of the deforming body may vary from very simple linear elastic models in small strain to highly complex nonlinear deformations of inelastic materials. Examples of deforming body–fluid interaction include aeroelasticity, biomedical applications and poroelasticity.

The interaction between fluid (incompressible or compressible) and solid (rigid or deformable) can be *strong* or *weak*, depending on how much a change in one domain influences the other. An example of weakly coupled problem is aeroelasticity at high Reynolds number, while incompressible flow often leads to strongly coupled problems. This distinction can lead to different solution strategies, as briefly described below.

Physical models aren't the only way in which FSI problems can be classified. The solution

procedure employed plays a key role in building models and algorithms to solve this kind of problems. The two main approaches are: the *monolithic approach* in which both fluid and solid are treated as one single system and the *partitioned approach* in which fluid and solid are considered as two separated systems coupled only through an interface. This latter approach is often preferred when building new solution procedures as it allows to use solvers that have been already developed, tested and optimized for a specific domain. The solvers only need to be linked to a third component, which takes care of all the interaction aspects.

The partitioned approach can be further classified considering the coupling between the fluid and solid: the solution may be carried out using a *weakly coupled approach*, in which the two solvers advance without synchronization, or a *strongly coupled approach*, in which the solution for all the physics must be synchronized at every time step. Although the weakly coupled approach is used in some aerodynamic applications, it is seldom used in other areas due to instability issues. A strongly coupled approach is generally preferred, even though this leads to more complex coupling procedures at the interface between fluid and solid.

This work describes the implementation and the validation of what is called an *adapter*, that is the "glue-code" needed to interface a solver to a coupling software library, thus adopting a *partitioned approach* to solve FSI problems. The *adapter* presented here connects the software code *MultiBody Dynamics analysis software (MBDyn)* to the multiphysics coupling library *precise Code Interaction Coupling Environment (preCICE)*.

Interfacing MBDyn with preCICE has multiple advantages: on one side it extends the capabilities of MBDyn to be used in FSI simulations by connecting it with a software library which has been already connected to widely used CFD solvers; on the other side, it allows to describe and simulate FSI problems with a suite of lumped, 1D and 2D elements (i.e. rigid bodies, *beams*, *membranes*, *shells*, etc.) decoupling the shape of the object (the interface with the fluid) from its structural properties, which can be described by different models and constitutive laws.

The thesis is structured as follows:

- Section 2 introduces the reader to FSI problems and their complexity, with particular attention to the physical description of the fluid and solid domains and the interface.
- Section 3 focuses on numerical methods, describing how to computationally deal with these kind of problems: details regarding the different coupling approaches are given here.
- Section 4 explains the features of preCICE that the adapter needs to support and gives a short introduction to MBDyn, explaining the main functionalities of interest.
- Section 5 presents the adapter developed in this work, its most important features and how to configure a FSI simulation with it.
- Section 6 describes the successful validation of the adapter, the comparison of the results with some well-known benchmarks and an example of real world application.
- Section 7 summarizes the findings and outcome of this work and gives an outlook to future work on this topic.
- Finally XX appendices give further information on...

Chapter 2

Physical aspects of Fluid-Structure Interaction problems

Dynamic models of solids or fluids aim at describing the evolution of an initial configuration through time. Structural mechanics and fluid dynamics use different perspectives when describing the motion of respectively a solid or a fluid particle. When dealing with FSI problems the two approaches need to be combined in order to obtain a suitable description of the two domains and their interface: this aspect is treated in 2.1.

As outlined in the introduction, the fluid and the solid domain of a FSI problem might be described by means of many different models: some of them are outlined in section 2.2. *Dimensional analysis* and the use of dimensionless numbers is a powerful tool used to classify fluid dynamics problems: some of the principles used there can be applied to FSI problems in order to classify them: this can help define and classify FSI problems, as described in section 2.3.

2.1 Description of motion

In a FSI model, the fluid in motion deforms the solid because of the forces exerted to the structure. The change in the shape of the solid modifies the fluid domain, causing a different flow behavior. For this reason it is necessary to describe formally the kinematics and the dynamics of the whole process. Classical continuum mechanics considers the motion of particles by means of two different perspectives [2]: the *Eulerian description*, briefly described in section 2.1.1, and the *Lagrangian description*, outlined in section 2.1.2. Those two perspectives are typically combined into the *arbitrary Lagrangian-Eulerian (ALE)* method, described in section 2.1.3.

2.1.1 Eulerian perspective

The *Eulerian perspective* observes the change of quantities of interest (e.g. density, velocity, pressure) at spatially fixed locations. In other words: the observer does not vary the point of view during different time steps. Thus, quantities can be expressed as functions of time at fixed locations. This is represented by the following notation:

$$\Theta = \tilde{\Theta}(x, y, z, t) \tag{2.1}$$

where Θ is a quantity of interest and $\tilde{\Theta}$ denotes the same quantity from an Eulerian point of view; (x, y, z) represent a fixed location in the euclidean space.

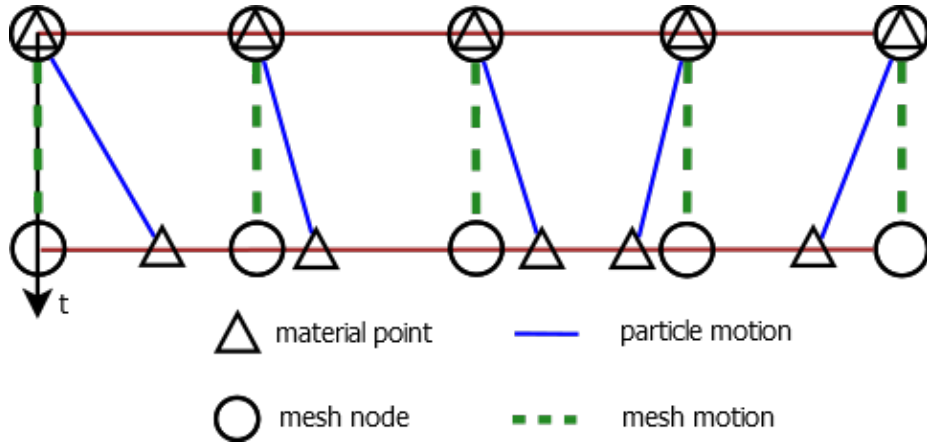


Figure 2.1. Eulerian perspective

A computational mesh can be interpreted as a number of observers distributed across the domain of interest and connected to each other in order to form a grid with nodes. If the particles of the domain move, a purely euclidean mesh does not move and the position other nodes remain fixed at any instance of time [3]. This behavior is represented in Figure 2.1 (adapted from [3]). The mesh is independent of particles movement, resulting in a convenient choice for Computational Fluid Dynamics (CFD) problems, where fluid flows throughout the whole computational domain. Within this approach, proper mesh refinement is crucial for computational accuracy as it defines to what extent small scale movement can be modeled and resolved [4].

2.1.2 Lagrangian perspective

A *lagrangian observer* focuses on a single particles and follows it throughout the motion, as depicted in Figure 2.2. Changes in the quantities of interest are observed at different spatial locations.

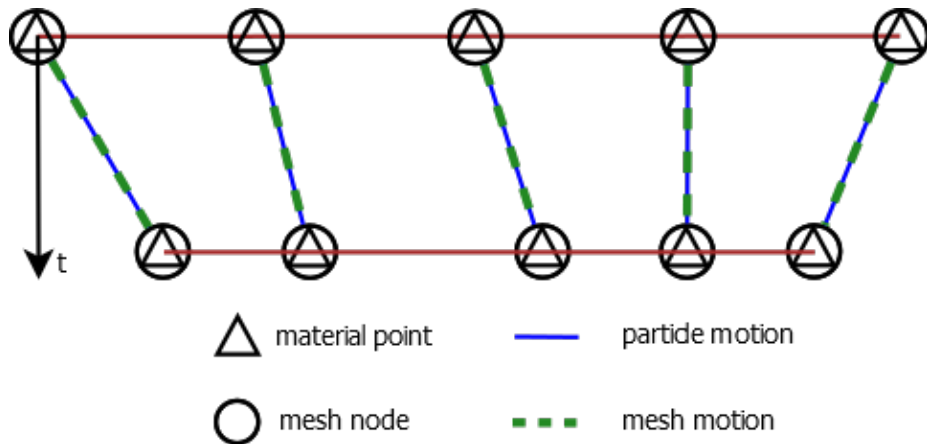


Figure 2.2. Lagrangian perspective

The motion of the particle and the other quantities of interest can be described by reference coordinates (or *material coordinates*) in Euclidean space (X, Y, Z) , uniquely identifying the observed particle at a reference configuration [5]. Usually $t = 0$ is chosen as reference but this

is not mandatory. The Lagrangian observer only registers changes concerning one specific particle as time advances. Thus, quantities of interest can be described as:

$$\Theta = \hat{\Theta}(X, Y, Z, t) \quad (2.2)$$

In contrast to the Eulerian perspective (Equation 2.1), the obtained information is strictly limited to a single material particle (implied by the usage of the capital reference coordinate variables). Information about a fixed point in space is not directly available and no convective fluxes appear in a Lagrangian description.

This perspective is again translated into computational meshes: at a reference instance of time, mesh nodes are attached to material particles. As these move, the mesh nodes move with them causing the mesh to deform. Figure 2.2 describes the situation. The mesh nodes always coincide with their respective particles.

In this situation large-scale and irregular motions and more importantly deformation lead to distortions of the computational mesh, which yields smaller accuracy in simulations requiring to apply techniques to keep the desired accuracy [6].

Lagrangian perspective is the usual method of choice for Computational Solid Mechanics (CSM) simulations.

Eulerian and Lagrangian descriptions are related [7]. A mapping between them can be described by the *motion* function ϕ such that:

$$\vec{x}(t) = \phi(\vec{X}, t) \quad (2.3)$$

Equation 2.3 tells that the Eulerian, spatial position \vec{x} of a particle at time t is the mapping of the particle at its reference configuration \vec{X} : the mapping must be bijective.

2.1.3 ALE method

As outlined above, CSM and CFD problems adopt different perspectives. The ALE approach, a combination of the two points of view, is used for FSI problems. As the name implies, an ALE observer moves arbitrarily with respect to a specific material particle. Figure 2.3 depicts such a situation.

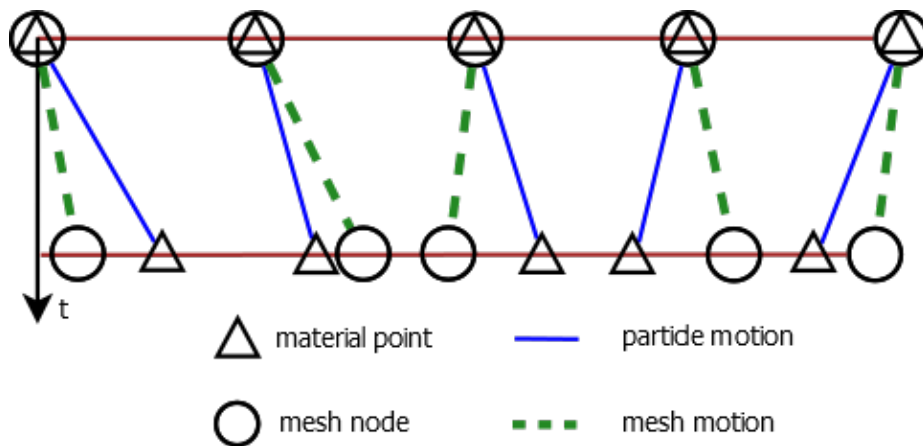
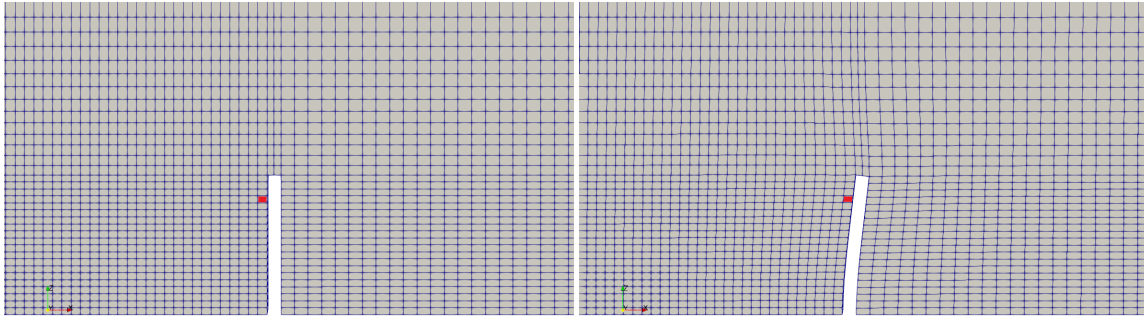


Figure 2.3. ALE perspective

When dealing with computational meshes, an ALE mesh is considered as it can move almost arbitrarily with respect to the motion of the underlying particles, as shown in Figure 2.4. The only constraint is that node movements should not distort the mesh too much

as this leads to computational inaccuracy. Many algorithm exist to implement suitable quality criteria and keep the mesh motion reasonable and to allow the nodes to follow moving particles up to a certain extent [8].

Since the mesh motion and material particle motion are not directly linked, a new unknown is introduced: the relative movement between the ALE mesh and the material domain. This approach is particularly useful in FSI problems: fluid and solid must follow the moving interface between them for physical reasons. Since the solid domain is usually described in a Lagrangian perspective, the solid mesh is kept attached to the FSI interface. However, also the fluid domain must deform to avoid formation of gaps between the meshes. Therefore, in ALE methods the fluid mesh nodes at the interface move with it. Fluid mesh nodes follow the fluid particles sticking to the interface (for viscous flows), while the rest of the fluid mesh is allowed to move in such way that mesh distortions are kept minimal, to preserve computational accuracy [9].



(a) undistorted mesh

(b) distorted mesh

Figure 2.4. ALE mesh

2.2 Domains and interface

Fluid-structure interaction implies that the overall model is determined by models defining the fluid behavior and the solid behavior, briefly described in sections 2.2.2 and 2.2.1. A short overview of beam models is given in section 2.2.3 as it is relevant for the model developed in this work. Finally a formal definition of the interface is given in section 2.2.4, as it is necessary to define suitable coupling conditions at the common boundary of the solid and the fluid.

2.2.1 Fluid domain

An exhaustive description of all possible fluid models is far beyond the scope of this work. A quite general model is the viscous compressible one described by the Navier Stokes Equations (NSE).

$$\frac{\partial \rho}{\partial t} + \nabla \cdot (\rho \vec{v}) = 0 \quad (2.4a)$$

$$\frac{\partial}{\partial t} (\rho \vec{v}) + \nabla \cdot (\rho \vec{v} \otimes \vec{v}) + \nabla p - \nabla \cdot \tau - \rho \vec{g} = 0 \quad (2.4b)$$

$$\frac{\partial}{\partial t} (\rho e_0) + \nabla \cdot (\rho e_0 \vec{v}) + \nabla \cdot (\vec{v} p + \vec{q} - \vec{v} \cdot \tau) - \vec{v} \cdot \rho \vec{g} = 0 \quad (2.4c)$$

where:

- ρ denotes density
- \vec{v} is flow velocity in all dimensions
- p denotes pressure
- $\boldsymbol{\tau}$ is the viscous stress tensor
- \vec{g} represents the sum of all body forces
- e_0 is the total energy per unit mass
- \vec{q} is the heat flux by conduction

They consist in the mass conservation equation (2.4a), the conservation of momentum equation (2.4b) and the energy conservation equation (2.4c). For a Newtonian fluid, the viscous stress tensor is given by:

$$\boldsymbol{\tau} = -\frac{2}{3}\mu (\nabla \cdot \vec{v}) \boldsymbol{I} + 2\mu \boldsymbol{S} \quad (2.5)$$

with μ being the dynamic viscosity and \boldsymbol{S} the rate of deformation tensor (i.e. the symmetric part of the velocity gradient $\nabla \vec{v}$):

$$\boldsymbol{S} = \frac{1}{2} (\nabla \vec{v} + \nabla \vec{v}^T) \quad (2.6)$$

A detailed derivation of such equations and the theory beyond can be found for example in [10] and [11] or in [12].

The set of equations above, even with a Newtonian fluid model, lack some other information in order to form a closed set of Partial Differential Equations (PDE). A conductive heat flux model is needed (e.g. Fourier's Law), the caloric and thermodynamic equations of state have to be chosen, a proper turbulence model if needed (see [12]) and finally, the appropriate initial and boundary conditions for the problem [13] must be defined.

Simplifications can be done to obtain less sophisticated models such as: adiabatic, inviscid, incompressible, and many others. Dimensional Analysis is a powerful tool to determine to what extent some reduced models are meaningful, and it is widely used in fluid dynamics, as described in section 2.3.1. Most CFD software codes allow to set up simulations with the most suitable model which can be coupled with a solid model to build a FSI problem. Some further details are given in section 3.1.

2.2.2 Solid domain

In solid mechanics, particles do not travel as much as they do in fluid dynamic problems, as described in 2.1.2. For this reason, a Lagrangian perspective is generally used.

The de-Saint Venant-Kirchhoff model [14] is very commonly used when describing the movement of a solid: it is also often used in FSI problems as it is capable of handling large deformation. The material is considered:

- *homogeneous*: the material properties do not depend on the position of the particle
- *linear elastic*: the stress-strain relationship is linear
- *isotropic*: the stress-strain relationship is independent from the direction of the load

A general expression of the dynamic equation can be derived from the Virtual Work Principle (VWP) applied to an arbitrary control volume:

$$\frac{\partial^2 \vec{u}}{\partial t^2} = \nabla \cdot \mathbf{T} + \rho \vec{f} \quad (2.7)$$

In equation 2.7:

- ρ : is the material density
- \vec{u} : is the particle displacement
- \mathbf{T} : is the *second Piola-Kirchhoff* stress tensor
- \vec{f} : is the sum of body forces

In order to close the dynamic equation, a constitutive law which must be considered to relate stress and strain:

$$\mathbf{T} = \lambda \mathbf{I} \text{tr} [\boldsymbol{\varepsilon}_G] + 2\mu \boldsymbol{\varepsilon}_G \quad (2.8)$$

where $\boldsymbol{\varepsilon}_G$ is the Green-Lagrange strain tensor:

$$\boldsymbol{\varepsilon}_G = \frac{1}{2} (\mathbf{F}^T \mathbf{F} - \mathbf{I}) \quad (2.9)$$

and \mathbf{F} is the deformation gradient. λ and μ are material properties and are named Lamé constants. These relate to the Young modulus E and the Poisson ratio ν which are more commonly used in practice. The relationship among the various parameters is the following:

$$E = \frac{\mu(3\lambda + 2\mu)}{\lambda + \mu} \quad (2.10)$$

$$\nu = \frac{\lambda}{2(\lambda + \mu)} \quad (2.11)$$

The set of parameters (E, ν) or (λ, μ) , together with the density ρ fully define the material, under the assumptions of linear elasticity, isotropy and homogeneity.

The set of PDEs is completed when suitable initial and boundary conditions are defined.

2.2.3 Models with reduced dimensionality: beams

The equations introduced in section 2.2.2 may be a tough task to solve even of the case of isotropic hyperelasticity, when considering a 3-D domain. Even with today's computers and using finite elements techniques, it is not always feasible or convenient to treat a solid as a three-dimensional continuum. Body with particular geometric features can be seen as lower dimension bodies, with respect to the governing equations [15]. Such bodies are called *beams* (one dimension) , *plates* or *shells* (two dimensions).

The *beam* model splits the description of the geometry into two subproblems:

1. a beam is defined by its *reference line* and the movement (displacement and rotation) of the solid is completely defined by it (see Figure 2.5),

- the beam *cross section* is considered as a whole, its movement depends on the movement of the reference line, stresses are generalized into *resultants* (axial, bending, shear, torsional) which represent the aggregate effect of all of the stresses acting on the cross section. The constitutive properties of the section (axial, shear, torsion and bending stiffness) allow to relate stresses and deformations (by means of VWP) and close the problem.

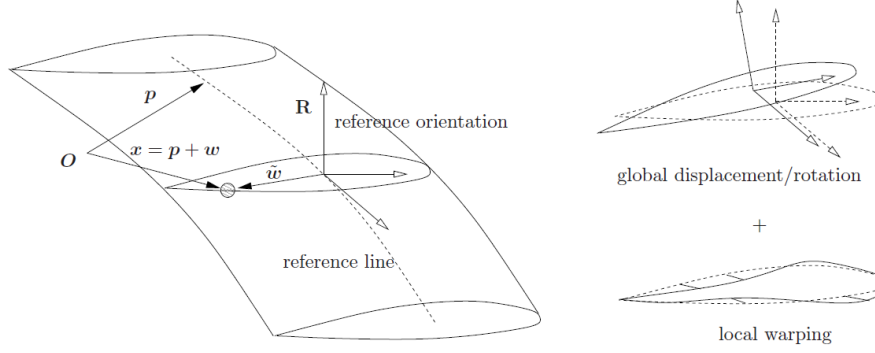


Figure 2.5. beam model, taken from [1]

The beam model can be used to build elements of a Finite Element Method (FEM). For example, the beam element can be modeled by means of a Finite Volume approach, as described in [16], which computes the internal forces as functions of the straining of the reference line and orientation at selected points along the line itself, called evaluation points.

This approach is particularly interesting for FSI problems in which slender structures are involved. A mapping is needed between the fluid-solid interface and the reference line movement, which will be described in.

2.2.4 Interface and interaction

Since FSI problems are centered on the interaction of the fluid and solid domain, their common interface needs to be described properly. A simple representation of the situation at the so called *wet surface* is shown in Figure 2.6. Quantities related to the solid use S subscript, while fluid domain and the interface are labeled with F and FS, respectively.

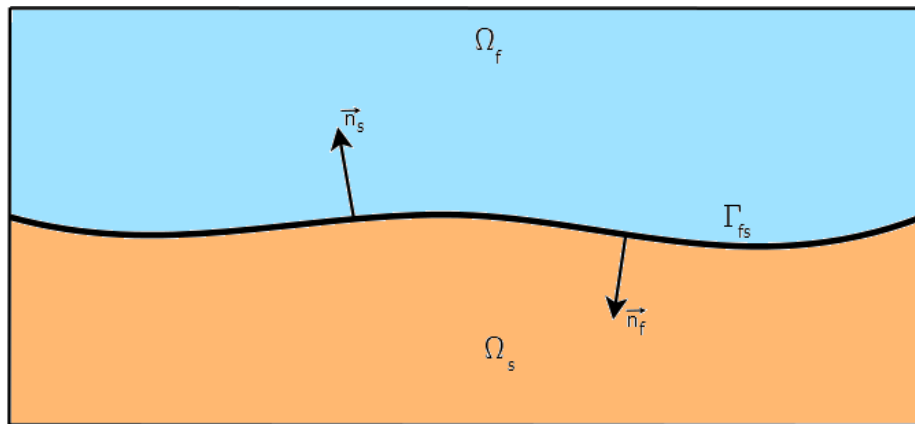


Figure 2.6. fluid solid interface

In order to have a physically correct behavior, some conditions have to be met [17]:

- solid and fluid domains should not overlap nor separate,
- for a viscous fluid model, the flow velocity at the interface must equal the boundary velocity (*no-slip* condition),
- for an inviscid fluid model, only velocity components normal to the wet surface have to be equal to the structural velocity as the fluid may slip freely in tangential direction at any boundary,
- forces exchanged at the interface must at equilibrium.

The first conditions result in the *kinematical requirement* that the displacements of fluid and solid domains, as well as their respective velocities have to be equal at the wet surface (denoted by Γ_{FS}):

$$\Delta \vec{x}_F = \vec{u}_S \quad (2.12)$$

$$\vec{v}_F = \frac{\partial \vec{u}_S}{\partial t} \quad (2.13)$$

The last condition results in the equilibrium requirement. Force vectors are computed from the stresses at the interface and the outward normal vectors of fluid and solid domain, respectively. They have to be equal and opposite leading to the dynamic coupling condition:

$$\boldsymbol{\sigma}_F \cdot \vec{n}_F + \boldsymbol{\sigma}_S \cdot \vec{n}_F = 0 \quad (2.14)$$

$\boldsymbol{\sigma} \in \mathbb{R}^{3 \times 3}$ represents the stress tensor (note that for the fluid it comprises pressure and viscous stresses), while $\vec{n} \in \mathbb{R}$ is the outward normal unit vector.

2.3 Classification of FSI problems

In the previous chapters we have seen that there exist a lot of models that can describe fluid flow and solid mechanics. In FSI problems we need to couple two of them: the variety of coupled problems seems to be so large that single FSI model that is applicable to every problem appears to be unfeasible. For this reason it is useful to classify FSI problems and look for specific properties in each class. The first step is to switch from dimensional quantities to dimensionless ones.

2.3.1 Dimensional analysis

We use the principle that a physical law should only relate to dimensionless quantities. There exist a rather general theorem called the Π Theorem or the *Vaschy-Buckingham Theorem* [18], which tells how many dimensionless quantities are needed to rewrite a model in dimensionless fashion. This theorem states that the number of dimensionless quantities, P , is equal to that of the dimensional ones describing the problem, N , minus R , which is the rank of the matrix of dimension exponents. This matrix is formed by the columns of the dimension exponents of all variables [19]. An example is given in the following Section 2.3.2, Table 2.1.

2.3.2 Dimensional analysis in fluid domain

Dimensional analysis is widely used in fluid dynamics. In order to keep the analysis simple, we consider the adimensionalization of the incompressible Navier-Stokes momentum equation for a Newtonian fluid [20]:

$$\frac{\partial \vec{v}}{\partial t} + (\vec{v} \cdot \nabla) \vec{v} = -\frac{\nabla p}{\rho} + \nu \nabla^2 \vec{v} + \vec{g} \quad (2.15)$$

The variables involved in equation 2.15 are the following:

- t : time
- \vec{x} : coordinates
- \vec{v} : velocity field
- p : pressure field
- ρ : fluid density
- ν : fluid kinematic viscosity
- \vec{g} : gravity
- L : reference dimension
- V_0 : reference velocity

	t	\vec{x}	\vec{v}	p	ρ	ν	\vec{g}	L	V_0
L	0	1	1	-1	-3	2	1	1	1
M	0	0	0	1	1	0	0	0	0
T	1	0	-1	-1	0	-1	-2	0	-1

Table 2.1. fluid matrix of dimension exponents

The rank of the above matrix is 3 so 6 dimensionless parameters are needed to rewrite the equation 2.15:

- *length*: $\vec{x}^* = \frac{\vec{x}}{L}$
- *velocity*: $\vec{v}^* = \frac{\vec{v}}{V_0}$
- *time*: $t^* = \frac{V_0 t}{L} = \frac{t}{T_{fluid}}$
- *pressure*: possible choices: $p^* = \frac{p}{\rho V_0^2}$ or, if viscous forces are dominant, $p^* = \frac{pL}{\rho \nu V_0}$
- *Reynolds number*: $Re = \frac{V_0 L}{\nu}$. It defines the ratio between inertia and viscous forces.
- *Froude number*: $Fr = \frac{V_0}{\sqrt{gL}}$. It defines the ratio between the flow inertia to the body field forces

The adimensionalized momentum equation becomes:

$$\frac{\partial \vec{v}^*}{\partial t^*} + (\vec{v}^* \cdot \nabla) \vec{v}^* = -\nabla p^* + \frac{1}{Re} \nabla^2 \vec{v}^* + \frac{1}{Fr^2} \vec{g} \quad (2.16)$$

From Equation 2.16 a lot of models might be derived: from *Stokes regime* when viscosity is dominant, to *Euler regime* when viscosity is negligible with respect to inertia forces.

2.3.3 Dimensional analysis in solid domain

Even if it is seldom used, Dimensional Analysis can be made also for the solid domain [21].

The variables involved in a solid dynamics equation are:

- t : time
- \vec{X} : coordinates
- \vec{u} : displacement field
- ρ_S : solid density
- E : elastic modulus
- \vec{g} : gravity
- L : reference dimension
- U_0 : reference displacement

From the variables above the following parameters can be derived:

- *length*: $\frac{\vec{X}}{L}$: dimensionless coordinate
- *displacement*: $\frac{\vec{u}}{L}$: dimensionless displacement
- *time*: $\frac{t\sqrt{\frac{E}{\rho_S}}}{L} = \frac{t}{T_{solid}}$ dimensionless time
- entity of displacements: $\frac{U_0}{L} = \delta$: *displacement number*
- gravity: $\frac{\rho_S g L}{E}$: elastogravity number

T_{solid} can be seen as $\frac{L}{c}$ with $c = \sqrt{\frac{E}{\rho_S}}$ which is the scale of elastic wave velocity. The displacement number δ tells how big the structure displacement are related to the overall dimension, and defines the *large displacements* region. Finally, the *elastogravity number* combines gravity (or body forces in general), density and stiffness: when large the deformation induced by body forces in the solid are large.

2.3.4 Dimensional analysis of coupled problems

It is now possible to undertake the dimensional analysis of a fully coupled fluid and solid interaction problem. Some of the parameters are only defined in the fluid side or in the solid side (e.g. viscosity or stiffness). Some parameters are common to both domains (e.g. length scale or gravity). The variables of interest are now the velocity in the fluid and the displacements in the solid. Each of them can be related to all the parameters without separation. For example, the fluid velocity relationship is of the kind:

$$g(\vec{v}; \vec{x}, t; \rho, \mu, V_0; \rho_S, E; \vec{g}, L) = 0 \quad (2.17)$$

Equation 2.17 is composed of 11 dimensional parameters. Applying π theorem, the total number of independent dimensionless parameter expected is 8. Starting from the ones derived in the previous sections:

- $\vec{x}^* = \frac{\vec{x}}{L}$: dimensionless coordinates
- $\vec{v}^* = \frac{\vec{v}}{V_0}$: dimensionless fluid velocity
- $t^*_f = \frac{V_0 t}{L}$: dimensionless time
- $Re = \frac{V_0 L}{\nu}$: Reynolds number
- $Fr = \frac{V_0}{\sqrt{gL}}$: Froude number
- $\delta = \frac{U_0}{L}$: displacement number
- $\frac{\rho_s g L}{E}$: elastogravity number

The 7 quantities above derive from the separated problem. The last one necessarily mixes things from the fluid and the solid side otherwise it would have been found in one uncoupled case. There is no unique choice for this parameter, the following are the most common ones.

Mass number

The simplest, but arguably most important parameter is the ratio of the two densities: the *Mass Number* M .

$$M = \frac{\rho}{\rho_s} \quad (2.18)$$

This can range from $\mathcal{O}(10^{-4})$ in air-steel interaction to $\mathcal{O}(1)$ when both media have about the same density. This parameter is particularly significant for the so called *added mass* stability problem, described in Section 3.5.

Reduced velocity

Another possible choice is the reduced velocity:

$$U_R = \frac{V_0}{\sqrt{\frac{E}{\rho_s}}} \quad (2.19)$$

It is the ratio between the fluid free velocity and the velocity of elastic waves in a solid, c . It contains information on the way the two dynamics are related and it can range different orders of magnitude.

Cauchy number

Another possible parameter combines stresses or stiffness: the Cauchy number, as defined in [22]:

$$C_Y = \frac{\rho V_0^2}{E} \quad (2.20)$$

It is the ratio between the fluid inertial forces, quantified by the dynamic pressure and the stiffness of the solid E . The higher it is, the more the solid is elastically deformed by the flow.

These are actually the most important parameters involving FSI problems. Among them, there is no universally better choice. But there are efficient choices, that would be more helpful in solving a given problem.

Chapter 3

Computational aspects of Fluid-Structure Interaction problems

This section deals with the computational aspects of FSI problems. The first possible categorization of solution techniques distinguishes between monolithic and partitioned approach, as discussed in Section 3.1. This work is based on the latter approach, so the two different coupling strategies, namely strong and weak, are discussed in Section 3.2. As strong coupling is generally needed for accurate solution, an overview of strong coupling algorithms is given in Section 3.3. Section 3.4 focuses on aspects concerning the interface mesh, and how the solid and the fluid exchange data between them. Finally 3.5 briefly describes a common issue arising in strongly coupled problems: the added mass effect (AME).

3.1 Monolithic and Partitioned Approach

Analytical solutions are impossible to obtain for the large majority of FSI problems; on the other hand, laboratory experiments may be costly, unfeasible or limited. For those reasons, numerical simulations may be employed to analyze the physics involved in the interaction between fluids and solids. With the current capabilities of computer technology, simulations of scientific and engineering models have become increasingly detailed and sophisticated.

The numerical methods used to solve FSI problems may be roughly classified into two classes: the *monolithic approach* and the *partitioned approach*. There is no exact distinction between the two approaches, as they might be seen differently among fields of applications. The idea here is to consider how many solvers are used to find a solution.

In the *monolithic approach*, the whole problem is treated as a unique entity and solved simultaneously with a specialized ad hoc solver (see Figure 3.1). The fluid and structure dynamics form a single system of equations for the entire problem, which is solved simultaneously by a unified algorithm. The interface conditions are implicit in the solution procedure [23], [24].

This approach can potentially achieve better accuracy, as they solve the system of equations exactly the interface conditions are implicit in the model [25], but it may require more resources and expertise to develop from scratch a specialized code (it solves a very specific model) that can be cumbersome to maintain.

On the other hand, in the *partitioned approach*, the fluid and the solid domains are treated as two distinct computational fields, with their respective meshes, that have to be solved separately (see Figure 3.2: how data are passed between solvers is detailed in Section 3.2). The interface conditions are used explicitly to communicate information between the

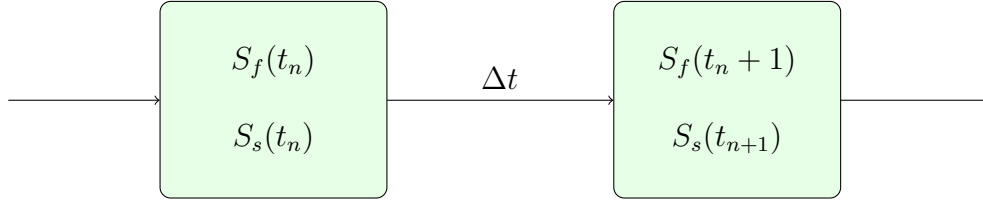


Figure 3.1. monolithic approach: S_f , S_s denote the fluid and the structure solutions

fluid and structure solutions. This implies that the flow does not change while the solution of the structural equations is calculated and vice versa [26]. The partitioned approach thus requires a third software module (i.e. a coupling algorithm) to incorporate the interaction aspects. It communicates the boundary conditions described in Section 2.2.4: that is forces or stresses (dynamic data) calculated by the fluid solver at the wet surface are passed to the solid component and displacements or velocities (kinematic data) computed by the solid solver at the interface are sent to the fluid component in return. Finally, fluid and structural solutions together yield the FSI solution.

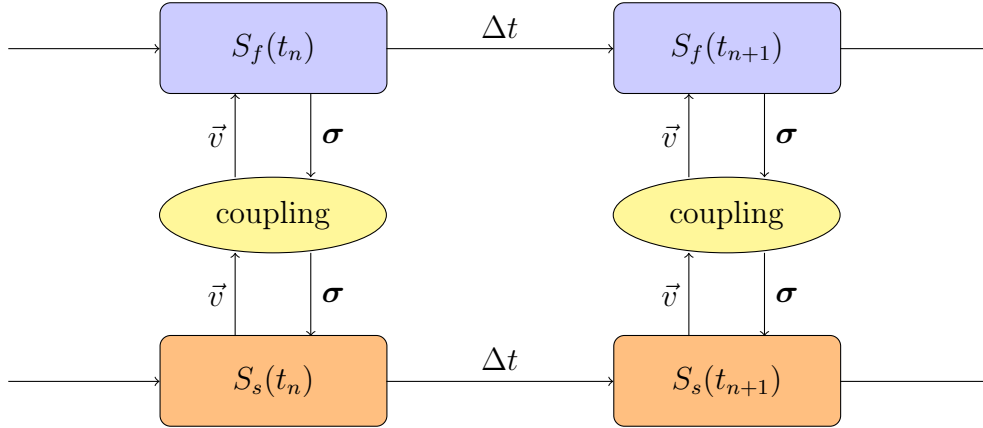


Figure 3.2. partitioned approach: S_f , S_s denote the fluid and the structure solutions, while σ and \vec{v} represent coupling data

A big advantage of this approach is that software modularity is preserved: different and efficient solution techniques can be used for the flow equations and structural equations. Provided that they can exchange data, existing solvers for the fluid and solid problem can be reused, ranging from commercial to academic and open-source codes. Those solvers are usually well-validated. Besides, compared to monolithic procedures, the programming efforts are lower for partitioned approaches, as only the coupling of the existing solvers has to be implemented rather than the solvers themselves. The challenge of this approach is, however, to define and implement algorithms to achieve accurate and efficient fluid-structure interaction solution with minimal code modification. Particularly, the interface location that divides the fluid and the structure domains changes in time. The partitioned approach requires that the fluid solver has ALE capabilities, as introduced in Section 2.1.3. More detailed and practical explanations about the coupling component used in this work are given in Section 4.1.

3.2 Coupling Strategies

Because of the modularity, the partitioned approach has gained much attention in research. The structure sketched in Figure 3.2 needs to be detailed and specialized in function of the coupling strategies.

In an interface multi-physics coupling like FSI, the boundary surface is in common between the two sides of the simulation. The results make sense and are numerically stable only if the two sides of the interface are in agreement, since the output values of the one simulation become input values for the other (and vice-versa). The solution strategies can be roughly divided into weakly and strongly coupled approaches. They are often referred to as *explicit* and *implicit* methods in the literature. When the fluid and solid solutions are computed iteratively until some convergence criteria within the same time step, the scheme is called *implicit coupling*. The faster, simpler but less precise *explicit coupling* consists in executing a fixed number of iterations (typically one per time step) and exchange coupling values without convergence checks.

3.2.1 Explicit coupling schemes

As in the previous Section, S_f represents the fluid solver, which computes the pressures (named d_f here) at the deformable boundary and S_s is the structure solver, which uses these forces to compute the displacement and velocity of the boundary (named d_s). In a *serial-explicit* (or *conventional staggered*) coupling scheme, the solver S_f uses the old time step boundary values $d_s^{(n)}$ to compute the values of $d_f^{(n+1)}$ for the next time step:

$$d_f^{(n+1)} = S_f \left(d_s^{(n)} \right) \quad (3.1)$$

When the fluid solver completes the time step, data are passed to the structural solver:

$$d_s^{(n+1)} = S_s \left(d_f^{(n+1)} \right) \quad (3.2)$$

Note that Equation 3.1 uses values computed at t^n , while Equation 3.2 uses values computed at $t^{(n+1)}$. The order of execution might be inverted.

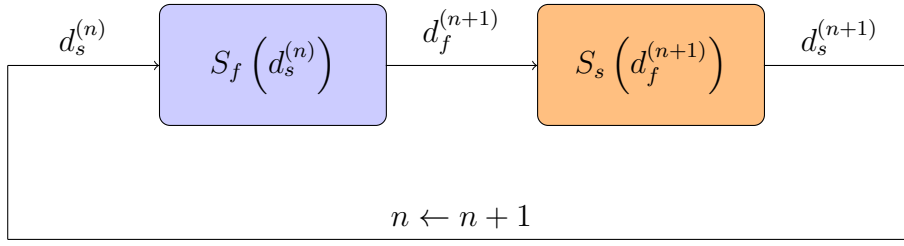
In order to reduce execution time, the solvers might run in parallel, using data from the same time step (*parallel-explicit coupling*):

$$d_f^{(n+1)} = S_f \left(d_s^{(n)} \right) \quad (3.3a)$$

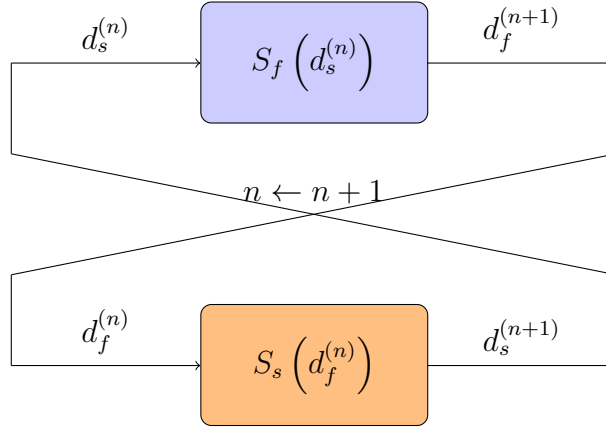
$$d_s^{(n+1)} = S_s \left(d_f^{(n)} \right) \quad (3.3b)$$

The two explicit schemes are shown schematically in Figures 3.3a and 3.3b.

In general, an explicit coupling is not enough to regain the exact (as in the monolithic approach) solution of the problem as the matching coupling conditions between the solvers is not enforced within each time step: no balance between fluid and structural domain with respect to forces and displacements at the interface can be guaranteed ([17], [26]). Nevertheless, explicit coupling yields good results if the interaction between fluid and solid is weak as in aeroelastic simulations, where in general the simulations show small displacements of the structure within a single time step and the flow field isn't much influenced by the structural displacements ([27]).



(a) serial explicit coupling



(b) parallel explicit coupling

Figure 3.3. Explicit coupling schemes

3.2.2 Implicit coupling schemes

On the other hand, strongly (implicit) coupling techniques require an iterative method to solve the fixed-point equation that derives from enforcing the agreement of the interface variables. The coupling conditions at the wet surface are enforced in each time step up to a convergence criterion. If the criterion is not met, another subiteration within the same time instance is computed. Therefore, the solution can approximate the monolithic solution to an arbitrary accuracy.

As in the explicit case, solvers may run in a sequential mode: the coupling is then named *serial* (or staggered) and the solvers wait for each other.

$$d_f^{(n+1),i+1} = S_f(d_s^{(n+1),i}) \quad (3.4a)$$

$$d_s^{(n+1),i+1} = S_s(d_f^{(n+1),i+1}) \quad (3.4b)$$

Equations 3.4 show that, in contrast with explicit coupling, both solvers use interface values at time step $n + 1$, but one of them uses data from previous iteration. If run in parallel mode [28], the system becomes:

$$d_f^{(n+1),i+1} = S_f(d_s^{(n+1),i}) \quad (3.5a)$$

$$d_s^{(n+1),i+1} = S_s(d_f^{(n+1),i}) \quad (3.5b)$$

At convergence, the following relation holds of serial (or *Gauss-Seidel*) coupling:

$$d_s^{(n+1)} = S_s \left(S_f \left(d_s^{(n+1)} \right) \right) \quad (3.6a)$$

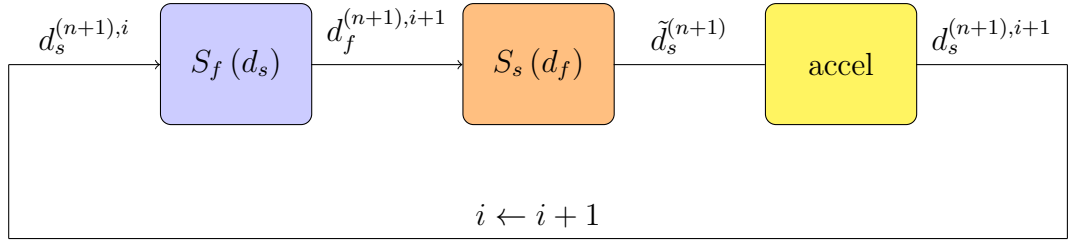
$$d_s^{(n+1)} = S_s \circ S_f \left(d_s^{(n+1)} \right) \quad (3.6b)$$

and the following relation holds for parallel (or *Jacobi*) coupling:

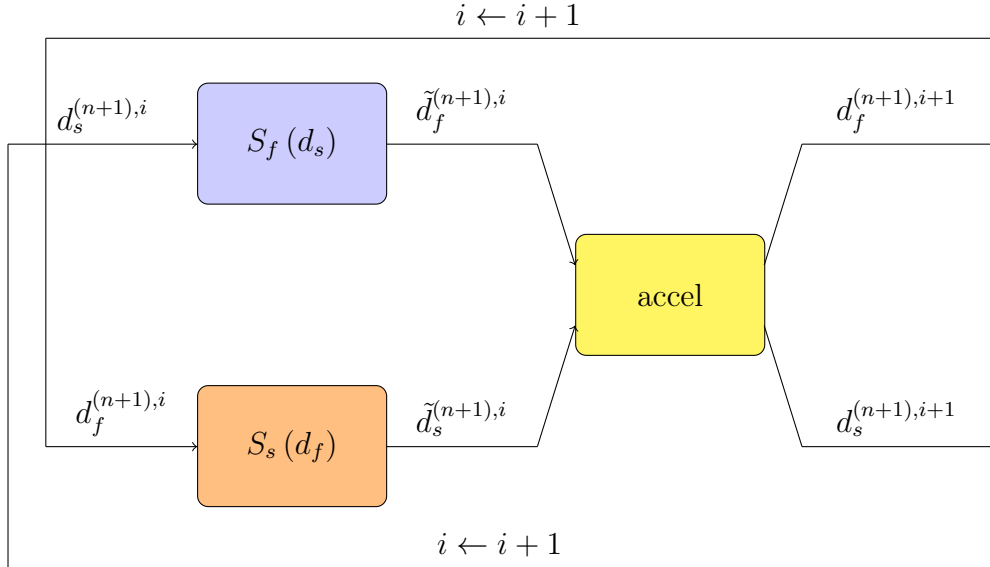
$$\begin{pmatrix} d_s^{(n+1)} \\ d_f^{(n+1)} \end{pmatrix} = \begin{pmatrix} 0 & S_f \\ S_s & 0 \end{pmatrix} \begin{pmatrix} d_s^{(n+1)} \\ d_f^{(n+1)} \end{pmatrix} \quad (3.7)$$

Acceleration techniques are necessary to bring fixed point equation 3.6b or 3.7 to convergence. Those techniques are described in Section 3.3.

The two implicit schemes are shown schematically in Figures 3.4a and 3.4b: *accel* refers to the post-processing step implemented to speedup convergence. After every non-converged iteration, the latest stored state of the solver (*checkpoint*) is reloaded and coupling iteration i for the current time step is incremented. When the solution converges, the time step n is incremented.



(a) serial implicit coupling



(b) parallel implicit coupling

Figure 3.4. Implicit coupling schemes

Implicit methods are generally applicable to any kind of FSI problems, in contrast with explicit methods. When fluid and structure are strongly coupled, explicit coupling can be

subject to numerical instabilities, a problem that cannot always be solved by reducing the coupling time step size [29]. These instabilities can be overcome by implicit methods, even if several coupling iterations may be executed every time step, until the values on both sides of the interface converge.

3.3 Strong coupling algorithms

As mentioned in the previous section, implicit methods require some post-processing (generally called *acceleration*) techniques to make the solution of the single time step of the coupled partitioned FSI problem converge. This requires to solve a *fixed-point equation*, in fact:

$$H(d_s) := S_s \circ S_f(d_s) \quad (3.8a)$$

$$d_s = H(d_s) \quad (3.8b)$$

$$R(d) := H(d) - d = 0 \quad (3.8c)$$

Equation 3.8a represents the composition of the solid and the fluid solution, while Equation 3.8b represents the resulting fixed point equation. As the order of execution can be switched, in Equation 3.8c, where the *residual* is defined, the input data d_s is generically substituted with d .

The basic approach to solve the fixed point equation is to perform the corresponding fixed point iteration (FPI):

$$x_{i+1} = H(x_i) \quad i = 1, 2, \dots \quad (3.9)$$

which is known to converge if the mapping H is a contraction, but this is not the general case in FSI computations [28].

3.3.1 under-relaxation

The way to stabilize the iterations is to perform a FPI with *under-relaxation* as illustrated in the following algorithm:

Algorithm 1: FPI with relaxation

Result: d_k

```

1 initialization of  $d_0$ ;
2  $k = 0$ ;
3  $\tilde{d}_1 = S_s \circ S_f(d_0)$ ;
4  $r_0 = \tilde{d}_1 - d_0$ ;
5 while  $\|r_k\| > \varepsilon$  do
6   | compute  $d_k$  by relaxation;
7   |  $k = k + 1$ ;
8 end
```

The under-relaxation is defined by:

$$d_{k+1} = d_k + \omega (H(d_k) - d_k) \quad (3.10)$$

Where ω in Equation 3.10 is the *relaxation factor*. The relaxation parameter has to be small enough to keep the iteration from diverging, but as large as possible in order to use as

much of the new solution as possible [30]. The optimal ω value is problem specific and not known a priori. A suitable dynamic relaxation parameter, is a better choice, like the *Aitken under-relaxation* [31] which adapts the factor at each iteration with the following relation:

$$\omega_i = -\omega_{i-1} \frac{r_{i-1}^T (r_i - r_{i-1})}{\|r_i - r_{i-1}\|^2} \quad (3.11)$$

Aitken under-relaxation can be a good choice for strong interaction with a fluid solvers that does not fully converge in every iteration or for compressible fluid solvers.

3.3.2 Quasi Newton Least Squares schemes

Under-relaxation is a good choice for easy stable problems, but is outperformed by more sophisticated quasi-Newton coupling schemes. Equation 3.8c could be solved iteratively with a Newton method [32]:

$$R(d_k) \quad := \quad r_k \quad (3.12a)$$

$$R(d_k) + \left. \frac{\partial R}{\partial d} \right|_{d_k} (d_{k+1} - d_k) = 0 \quad (3.12b)$$

$$d_k + \left(\left. \frac{\partial R}{\partial d} \right|_{d_k} \right)^{-1} (-r_k) = d_{k+1} \quad (3.12c)$$

The *residual* at iteration k is defined in Equation 3.12a, if the Jacobian matrix of the equation is known, a Newton iteration can be performed as in Equation 3.12b. The updated values can be computed using Equation 3.12c.

In situations where:

- *black-box* systems are considered (i.e. the Jacobian is unknown),
- the cost of a function evaluation is sufficiently high that numerical estimation of the Jacobian is prohibitive,

there exist a number of matrix-free methods that use only information derived from the consecutive iterates and that build an approximation based on those values. This approach is known as *quasi-Newton method* [33]. Input and output data of H and R are used to approximate the solution of 3.12c. Algorithm 12 (taken from [34]) shows the basics steps to

estimate data at next step using the *Quasi Newton Least Squares Method*:

Algorithm 2: Quasi Newton Least Squares method

Result: d_{k+1}

- 1 initial value d_0 ;
- 2 $\tilde{d}_0 = H(d_0)$ and $R_0 = \tilde{d}_0 - d_0$;
- 3 $d_1 = d_0 + \omega r_0$;
- 4 **for** $k = 1 \dots$ **do**
- 5 $\tilde{d}_k = H(d_k)$ and $r^k = \tilde{d}_k - d_k$;
- 6 $V^k = [\Delta r_0^k, \dots, \Delta r_{k-1}^k]$ with $\Delta r_i^k = r^i - r^k$;
- 7 $W^k = [\Delta \tilde{d}_0^k, \dots, \Delta \tilde{d}_{k-1}^k]$ with $\Delta \tilde{d}_i^k = \tilde{d}_i - d_k$;
- 8 decompose $V^k = Q^k U^k$;
- 9 solve the first k lines of $U^k \alpha = -Q^{kT} R^k$;
- 10 $\Delta \tilde{d}^k = W^k \alpha$;
- 11 $d_{k+1} = \tilde{d}_k + \Delta \tilde{d}_k$;
- 12 **end**

In algorithm 12 the matrices V^k and W^k are constructed from the previous iterations and the known values of d_0, \dots, d_k and $\tilde{d}_0, \dots, \tilde{d}_k$. $\Delta \tilde{d}^k$ is constructed in the column space of W^k (line 10). For this reason a least squares problem is solved:

$$\alpha = \underset{\beta \in \mathbb{R}^k}{\operatorname{argmin}} \|V^k \beta + R(d_k)\| \quad (3.13)$$

The least squares problem is solved computing the decomposition of V^k into an orthogonal matrix $Q^k \in \mathbb{R}^{k \times k}$ and an upper triangular matrix $U^k \in \mathbb{R}^{n \times k}$ (line 8). Then α is computed in line 9.

When building matrices V^k and W^k (lines 6-7), it is possible to use information from previous time steps.

Finally, to ensure linear independence of columns in the multi-secant system for Jacobian estimation, a filter can be used [35], in order to drop nearly dependent columns of Q^k and avoid singularity of the approximated Jacobian.

The above algorithm is usually denominated in FSI interface quasi Newton with inverse Jacobian from a least squares model (IQN-ILS) (or Anderson acceleration). There exist other algorithms, like generalized Broyden (IQN-IMVJ) or manifold mapping to solve the problem. A complete description of those methods goes beyond the scope of this work: a description of the most common algorithms can be found in [36], while a comparison of the performances can be found in [37].

3.3.3 Convergence criteria

At each time step, the coupling algorithm enforce matching conditions at the wet surface up to a convergence criterion. If not sufficiently met, another iteration within the same time step is performed. The fixed point formulation itself induces a criterion based on the residual itself r_{k+1} .

A scalar, *absolute convergence criterion* can be defined as in Equation 3.14: it is useful for close to zero values of the coupling quantities, when rounding errors become important:

$$\|r_{k+1}\| \leq \epsilon_{abs} \quad (3.14)$$

A more common *relative convergence criterion*, defined in Equation 3.15 is particularly useful when different quantities (e.g. forces and displacements) are compared together to evaluate convergence:

$$\frac{\|r_{k+1}\|}{\|\tilde{d}_{k+1}\|} \leq \epsilon_{rel} \quad (3.15)$$

3.4 Interface Mesh and Data Mapping

FSI methods can also be classified considering how the fluid and solid meshes are treated. The *conforming mesh methods* consider the interface as a physical boundary condition (see Section 3.4.2), while *non-conforming mesh methods* treat the boundary location as a constraint imposed on the model equations (see Section 3.4.1) [17].

3.4.1 Non-conforming Mesh methods

In non-conforming mesh strategies all interface conditions are imposed as constraints on the flow and structural governing equations. It is possible to use non-conforming meshes for fluid and solid domains as they remain geometrically independent from each other (see Figure 3.5).

This approach is mostly used in *immersed boundary* methods [38]. Coupling is imposed by means of additional force terms appearing in the model equations of the fluid, which impose the kinematic and dynamic conditions. The forces represent the effects of a boundary or body being immersed in the fluid domain. A purely Eulerian mesh (see Section 2.1.1) can be used for the whole computational domain, since the force terms are dynamically added at specific locations to represent the structure.

The fluid forces applied on the solid at the wet surface are computed and used as input for the structural solver, which employs a standard Lagrangian mesh (see Section 2.1.2).

Immersed boundary methods are particularly innovative and are useful to overcome some issues in CFD computations, on the other hand most of the current implementations of FSI problem implement a conforming mesh strategy.

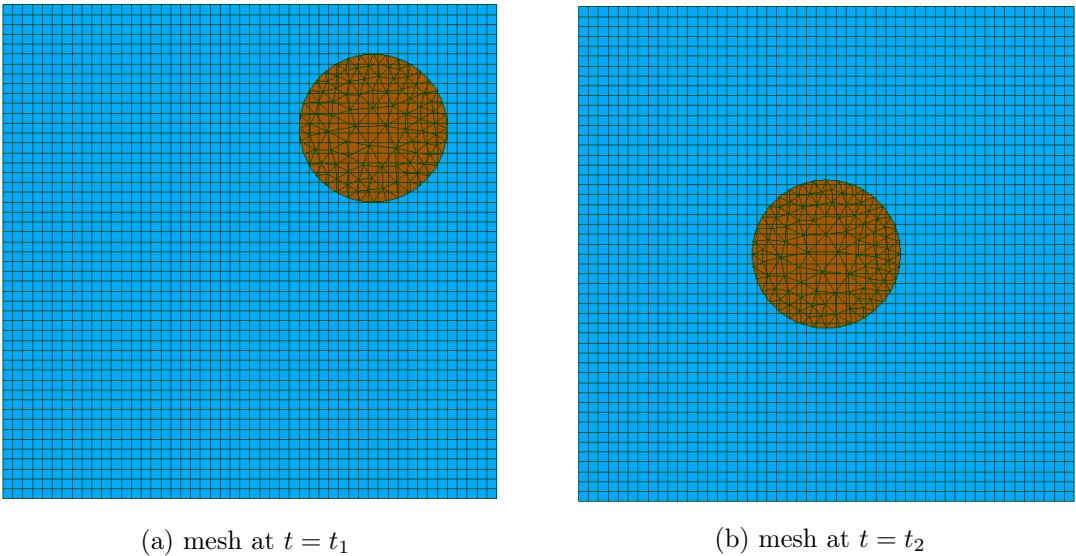


Figure 3.5. non conforming mesh example

3.4.2 Conforming Mesh methods

Conforming mesh methods adapt very well to the partitioned approach described in Section 3.1 as they usually consists in the computational steps described above, namely: computation in the fluid, computation in the solid, enforcing of interface condition and mesh movement (see Figure 3.6).

Fluid and structure meshes need share the boundary of the wet surface, as the coupling conditions are enforced by applying kinematic or dynamic conditions to those boundaries. Node-to-node matching of fluid and structure meshes at the interface is not required, as long as a suitable mapping between the interface nodes is performed (see Section 3.4.3).

The match between the interfaces must hold at each time step: this implies that both solid and fluid domains need to deform. Deformation is easily expressed in the solid domain as the structural mesh is usually represented in Lagrangian perspective (see Section 2.1.2). ALE perspective (Section 2.1.3) for the fluid domain becomes necessary in this case.

Mesh deformation can turn out to be a complicated task as in general the fluid mesh is deformed during motion (see Figure 2.4). Mesh smoothing techniques need to be applied in order to keep a good mesh quality in terms of distorted elements which can lead to accuracy loss in simulations. (the following video shows high distorted fluid elements during FSI motion: video).

Mesh smoothing is generally applied to keep the fluid mesh as uniform and undistorted as possible during movement. There is a wide variety of mesh updating procedures [39]. The *torsional spring analogy* [40] is a fairly simple technique that computes mesh movement considering mesh edges as springs and solving the subsequent Laplace equation that derives from the mesh movement.

Some other references about mesh motion alternatives can be found in [41].

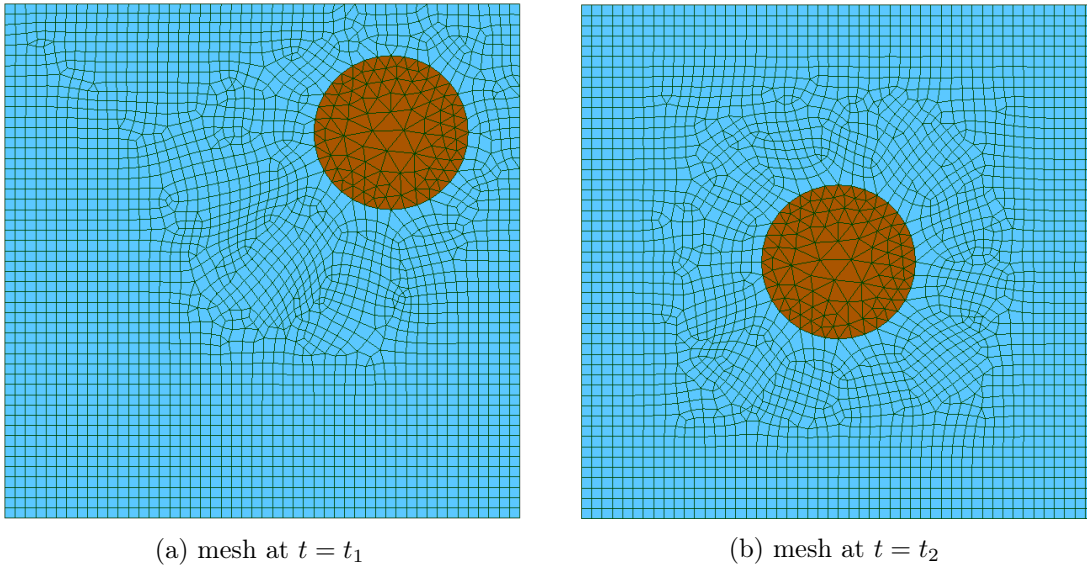


Figure 3.6. conforming mesh example

3.4.3 Data Mapping

When partitioned coupling is involved and the meshes are conforming but not node-to-node coincident, the challenge is to correctly map the data between the solid and the fluid sides.

This is a common situation as fluid and solid require a different mesh refinement at the interface.

The mapping procedure needs not only to find the closest available mesh point (or points) on the opposite mesh, but also to preserve mass and energy balance. Variables are basically mapped in two ways: *consistent* and *conservative* forms.

In the *consistent mapping* a value on a node of one grid has the same value of the corresponding node on another grid: that is, it reproduces the values on both meshes. In the *conservative form*, integral values are preserved between meshes. In an FSI problem, nodal forces are mapped in conservative form, while velocities or displacements are mapped in consistent form. An example is shown in Figure 3.7.

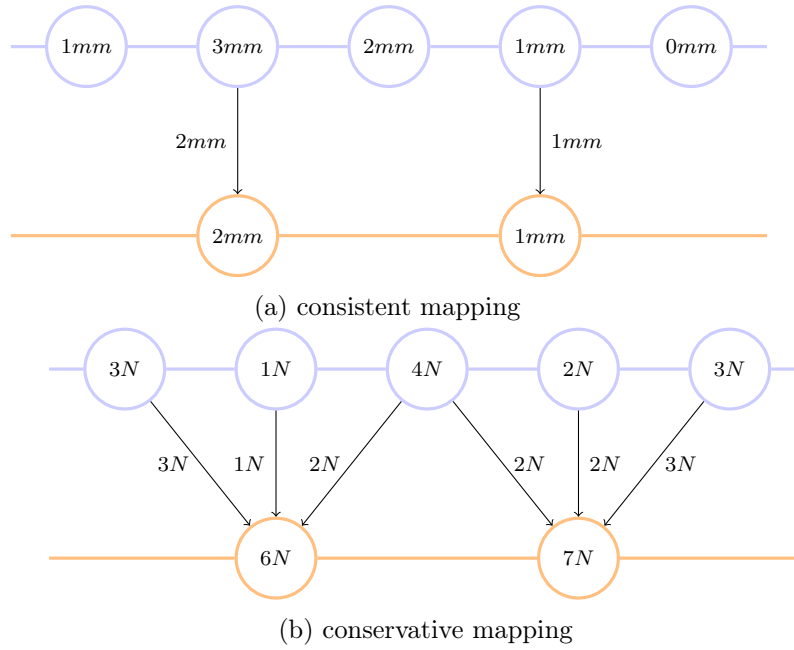


Figure 3.7. Examples of mapping data between non-coincident meshes: consistent (a) and conservative (b) schemes.

different mapping strategies can be implemented [42]:

- *Nearest Neighbor*: finds the closest point on the source mesh and uses its value for the target mesh. It does not require any topological information and is first-order accurate. It is the computationally easiest implementation and it is useful when interface meshes are coincident.
- *Nearest Projection*: projects the points of the target mesh on the source mesh, interpolates the data linearly and assigns the values to the target mesh. It requires topology information for the source mesh. The interpolation on the mesh elements is second order accurate.
- *Radial Basis Function (RBF)*: this method does not requires topological information and works well on general meshes. The mapping uses radial basis functions centered at the grid points of the source mesh [43].

3.5 Stability: Added Mass Effect

[29] [44] [45] [46]

To conclude this chapter about computational aspects of FSI simulations, the AME is briefly described. Explanations of this effect can be found in a great variety throughout FSI literature, typically explicated for specific solver strategies or flow regimes (see e.g. [5], [42], [15], [2]). Therefore, in the scope of this thesis only a short phenomenological introduction to the concept of added mass and numerical problems arising from it is given. However, this suffices to focus on both weakly and strongly coupled partitioned approaches, which are practically relevant in this thesis. The AME is inherent to partitioned FSI approaches as the single-physics fields are not continuously coupled but interaction only occurs at a finite number of discrete time instances, when coupling quantities are exchanged. As already mentioned in Section 2.3.3, there can be no gaps between structure and fluid. Also their respective particles cannot occupy the same spatial locations simultaneously. Thus, if the solid is moved, also fluid particles move. Changing the state of motion of the structural component consequently requires taking into account inertial effects not only of the solid itself, but also of the surrounding fluid, which artificially rests for the span of a single structure solver time step. In more descriptive words: Moving the solid also implies moving fluid particles close to the solid. Therefore, the structure behaves more inert due to artificially added mass ([42], [2]). Since inertia is dependent on mass and therefore density, the ([42], [5]): This ratio is often used to describe how strong the interaction between solid and fluid is. For cases, in influence the FSI problem (weak interaction). But as fluid and structure densities approach each other interaction) and imposes stability limits on partitioned solution techniques ([5], [42], [2]). Note that the AME is not only governed by the density ratio of Equation 3.1 but also by geometric properties of the problem, the stiffness of the solid ([5]) and the speed of sound in the flow domain ([42]). Nonetheless, for the sake of simplicity and intuitiveness, explanations in this thesis are mostly limited to the density ratio. In general, the AME is of bigger concern for incompressible flows than for compressible regimes. From a physical point of view, deformations of the structural domain can be interpreted as perturbations for the flow field. In compressible flows the speed of sound (speed at which perturbations propagate through the flow) is finitely large. Thus, the influence of a geometrical change of the fluid domain caused by deformations of the solid is locally limited during a certain period of time. In contrast, in incompressible flows the speed of sound is infinitely large, hence all perturbations propagate through the flow without time delay. Therefore, regardless of how much time has passed since a perturbation, the whole flow field is directly affected ([42], [5]). In the following it is assumed that a weakly coupled algorithm allows computation of the fluid and solid solution only once per time step. In addition, coupling data is also exchanged once per time instance. In contrast, a strongly coupled solver does the same at least twice per time increment (for a reminder see Section 3.2 and compare Figure 3.4). As can be shown, in the compressible case a more dominant AME can be compensated for by reducing the time step size of strongly coupled, partitioned solution algorithms. This however, does not hold for the incompressible regime, where even in the limit of vanishing time step size strongly coupled, partitioned algorithms might fail ([42]). These observations are consistent with the above mentioned physical explanation. First of all, considering compressible flows, indeed, the lack of repeated subiterations in weakly coupled partitioned techniques leads to a strict limit for the density ratio (of Equation 3.1) due to the fact that the interface conditions are not enforced and energy balance at the wet surface is generally not given. If that limit is exceeded the algorithm fails due to instability ([2]). Likewise, in such a case a strongly coupled partitioned algorithm converges slowly, resulting in possibly many necessary subiterations, which is computationally costly. Yet it does not become unstable, given that the time step size is chosen sufficiently small. Reducing the time step size to an arbitrarily small extent cannot stabilize a weakly coupled approach if the stability criterion on the density ratio is not met ([15]). Conversely, the convergence rate

of strongly coupled algorithms increases by the same factor, by which the time step size decreases, meaning that in the limit of vanishing time step size the monolithic solution is obtained ([5], [42]). In the incompressible case however, a strict stability limit exists for both weakly and strongly coupled algorithms. It is independent of the size of time increments¹. Furthermore, in order for an implicit method to achieve the monolithic solution (assuming its convergence is given, i.e. the before mentioned stability limit is not exceeded) the number of subiterations must be increased as time step size decreases ([15], [42]).

Chapter 4

Software Packages used in this work

Lorem ipsum dolor sit amet, consectetur adipiscing elit, sed eiusmod tempor incididunt ut labore et dolore magna aliqua. Ut enim ad minim veniam, quis nostrum exercitationem ullam corporis suscipit laboriosam, nisi ut aliquid ex ea commodi consequatur. Quis aute iure reprehenderit in voluptate velit esse cillum dolore eu fugiat nulla pariatur.

4.1 preCICE

[47] Official adapters

Chapter 5

MBDyn Adapter and its integration

Lorem ipsum dolor sit amet, consectetur adipiscing elit, sed eiusmod tempor incididunt ut labore et dolore magna aliqua. Ut enim ad minim veniam, quis nostrum exercitationem ullam corporis suscipit laboriosam, nisi ut aliquid ex ea commodi consequatur. Quis aute iure reprehenderit in voluptate velit esse cillum dolore eu fugiat nulla pariatur.

Chapter 6

Validation Test-cases

Lorem ipsum dolor sit amet, consectetur adipiscing elit, sed eiusmod tempor incididunt ut labore et dolore magna aliqua. Ut enim ad minim veniam, quis nostrum exercitationem ullam corporis suscipit laboriosam, nisi ut aliquid ex ea commodi consequatur. Quis aute iure reprehenderit in voluptate velit esse cillum dolore eu fugiat nulla pariatur.

Conclusions

35

[illegible]

ut labore et dolore magna aliqua. Ut enim ad minim veniam, quis nostrum exercitationem ullam corporis suscipit laboriosam, nisi ut aliquid ex ea commodi consequatur. Quis aute iure reprehenderit in voluptate velit esse cillum dolore eu fugiat nulla pariatur. Excepteur sint obcaecat cupiditat non proident, sunt in culpa qui officia deserunt mollit anim id est laborum. Lorem ipsum dolor sit amet, consectetur adipisci elit, sed eiusmod tempor incidunt ut labore et dolore magna aliqua. Ut enim ad minim veniam, quis nostrum exercitationem ullam corporis suscipit laboriosam, nisi ut aliquid ex ea commodi consequatur. Quis aute iure reprehenderit in voluptate velit esse cillum dolore eu fugiat nulla pariatur. Excepteur sint obcaecat cupiditat non proident, sunt in culpa qui officia deserunt mollit anim id est laborum. Lorem ipsum dolor sit amet, consectetur adipisci elit, sed eiusmod tempor incidunt ut labore et dolore magna aliqua. Ut enim ad minim veniam, quis nostrum exercitationem ullam corporis suscipit laboriosam, nisi ut aliquid ex ea commodi consequatur. Quis aute iure reprehenderit in voluptate velit esse cillum dolore eu fugiat nulla pariatur. Excepteur sint obcaecat cupiditat non proident, sunt in culpa qui officia deserunt mollit anim id est laborum. Lorem ipsum dolor sit amet, consectetur adipisci elit, sed eiusmod tempor incidunt ut labore et dolore magna aliqua. Ut enim ad minim veniam, quis nostrum exercitationem ullam corporis suscipit laboriosam, nisi ut aliquid ex ea commodi consequatur. Quis aute iure reprehenderit in voluptate velit esse cillum dolore eu fugiat nulla pariatur. Excepteur sint obcaecat cupiditat non proident, sunt in culpa qui officia deserunt mollit anim id est laborum. Lorem ipsum dolor sit amet, consectetur adipisci elit, sed eiusmod tempor incidunt ut labore et dolore magna aliqua. Ut enim ad minim veniam, quis nostrum exercitationem ullam corporis suscipit laboriosam, nisi ut aliquid ex ea commodi consequatur.

First Appendix

39

Appendix A. First Appendix

ut labore et dolore magna aliqua. Ut enim ad minim veniam, quis nostrum exercitationem ullam corporis suscipit laboriosam, nisi ut aliquid ex ea commodi consequatur. Quis aute iure reprehenderit in voluptate velit esse cillum dolore eu fugiat nulla pariatur. Excepteur sint obcaecat cupiditat non proident, sunt in culpa qui officia deserunt mollit anim id est laborum. Lorem ipsum dolor sit amet, consectetur adipisci elit, sed eiusmod tempor incidunt ut labore et dolore magna aliqua. Ut enim ad minim veniam, quis nostrum exercitationem ullam corporis suscipit laboriosam, nisi ut aliquid ex ea commodi consequatur. Quis aute iure reprehenderit in voluptate velit esse cillum dolore eu fugiat nulla pariatur. Excepteur sint obcaecat cupiditat non proident, sunt in culpa qui officia deserunt mollit anim id est laborum. Lorem ipsum dolor sit amet, consectetur adipisci elit, sed eiusmod tempor incidunt ut labore et dolore magna aliqua. Ut enim ad minim veniam, quis nostrum exercitationem ullam corporis suscipit laboriosam, nisi ut aliquid ex ea commodi consequatur. Quis aute iure reprehenderit in voluptate velit esse cillum dolore eu fugiat nulla pariatur. Excepteur sint obcaecat cupiditat non proident, sunt in culpa qui officia deserunt mollit anim id est laborum.obcaecat cupiditat non proident, sunt in culpa qui officia deserunt mollit anim id est laborum. Lorem ipsum dolor sit amet, consectetur adipisci elit, sed eiusmod tempor incidunt ut labore et dolore magna aliqua. Ut enim ad minim veniam, quis nostrum exercitationem ullam corporis suscipit laboriosam, nisi ut aliquid ex ea commodi consequatur.

Acronyms

FSI	Fluid-Structure Interaction
MBDyn	MultiBody Dynamics analysis software
preCICE	precise Code Interaction Coupling Environment
ALE	arbitrary Lagrangian-Eulerian
CFD	Computational Fluid Dynamics
CSM	Computational Solid Mechanics
NSE	Navier Stokes Equations
PDE	Partial Differential Equations
VWP	Virtual Work Principle
FEM	Finite Element Method
AME	added mass effect
FPI	fixed point iteration
IQN-ILS	interface quasi Newton with inverse Jacobian from a least squares model
RBF	Radial Basis Function

Bibliography

- [1] G. L. Ghiringhelli, P. Masarati, M. Morandini, and D. Muffo, “Integrated aeroservoelastic analysis of induced strain rotor blades,” *Mechanics of Advanced Materials and Structures*, vol. 15, no. 3-4, pp. 291–306, 2008.
- [2] R. C. Batra, *Elements of continuum mechanics*. Aiaa, 2006.
- [3] J. Cheng, G. Zhao, Z. Jia, Y. Chen, S. Wang, and W. Wen, “Sliding free lagrangian-eulerian finite element method,” in *International Conference on Computational Science*, 2006.
- [4] J. Donea, A. Huerta, J.-P. Ponthot, and A. Rodríguez-Ferran, “Arbitrary lagrangian-eulerian methods,” *Encyclopedia of Computational Mechanics Second Edition*, pp. 1–23, 2017.
- [5] J. T. Xing, “Chapter 3 - fundamentals of continuum mechanics,” in *Fluid-Solid Interaction Dynamics*, J. T. Xing, Ed. Academic Press, 2019, pp. 57 – 101. [Online]. Available: <http://www.sciencedirect.com/science/article/pii/B9780128193525000033>
- [6] S. Lipton, J. A. Evans, Y. Bazilevs, T. Elguedj, and T. J. Hughes, “Robustness of isogeometric structural discretizations under severe mesh distortion,” *Computer Methods in Applied Mechanics and Engineering*, vol. 199, no. 5-8, pp. 357–373, 2010.
- [7] A. Bertram, *Elasticity and plasticity of large deformations*. Springer, 2012.
- [8] A. De Boer, M. Van der Schoot, and H. Bijl, “Mesh deformation based on radial basis function interpolation,” *Computers & structures*, vol. 85, no. 11-14, pp. 784–795, 2007.
- [9] E. Ramm and W. Wall, “Fluid-structure interaction based upon a stabilized (ale) finite element method,” in *4th World Congress on Computational Mechanics: New Trends and Applications*, CIMNE, Barcelona, 1998, pp. 1–20.
- [10] L. Quartapelle and F. Auteri, *Fluidodinamica incompressibile*. Casa editrice ambrosiana, 2013.
- [11] —, *Fluidodinamica comprimibile*. Casa editrice ambrosiana, 2013.
- [12] S. B. Pope, “Turbulent flows,” 2001.
- [13] G. Galdi, *An introduction to the mathematical theory of the Navier-Stokes equations: Steady-state problems*. Springer Science & Business Media, 2011.
- [14] R. W. Ogden, *Non-linear elastic deformations*. Courier Corporation, 1997.
- [15] K. D. Hjelmstad, *Fundamentals of structural mechanics*. Springer Science & Business Media, 2007.

- [16] G. L. Ghiringhelli, P. Masarati, and P. Mantegazza, “Multibody implementation of finite volume c beams,” *AIAA journal*, vol. 38, no. 1, pp. 131–138, 2000.
- [17] G. Hou, J. Wang, and A. Layton, “Numerical methods for fluid-structure interaction—a review,” *Communications in Computational Physics*, vol. 12, no. 2, pp. 337–377, 2012.
- [18] H. Hanche-Olsen, “Buckingham’s pi-theorem,” *NTNU*: <http://www.math.ntnu.no/~hanche/notes/buckingham/buckingham-a4.pdf>, 2004.
- [19] J.-D. Hardtke, “On buckingham’s π -theorem,” *arXiv preprint arXiv:1912.08744*, 2019.
- [20] R. W. Fox, A. T. McDonald, and J. W. Mitchell, *Fox and McDonald’s introduction to fluid mechanics*. John Wiley & Sons, 2011.
- [21] S. Longo, *Analisi Dimensionale e Modellistica Fisica: Principi e applicazioni alle scienze ingegneristiche*. Springer Science & Business Media, 2011.
- [22] E. De Langre, *Fluides et solides*. Editions Ecole Polytechnique, 2001.
- [23] B. Hübner, E. Walhorn, and D. Dinkler, “A monolithic approach to fluid–structure interaction using space–time finite elements,” *Computer methods in applied mechanics and engineering*, vol. 193, no. 23-26, pp. 2087–2104, 2004.
- [24] P. Ryzhakov, R. Rossi, S. Idelsohn, and E. Oñate, “A monolithic lagrangian approach for fluid–structure interaction problems,” *Computational mechanics*, vol. 46, no. 6, pp. 883–899, 2010.
- [25] T. Richter, *Fluid-structure interactions: models, analysis and finite elements*. Springer, 2017, vol. 118.
- [26] J. Degroote, K.-J. Bathe, and J. Vierendeels, “Performance of a new partitioned procedure versus a monolithic procedure in fluid–structure interaction,” *Computers & Structures*, vol. 87, no. 11-12, pp. 793–801, 2009.
- [27] C. Farhat, K. G. Van der Zee, and P. Geuzaine, “Provably second-order time-accurate loosely-coupled solution algorithms for transient nonlinear computational aeroelasticity,” *Computer methods in applied mechanics and engineering*, vol. 195, no. 17-18, pp. 1973–2001, 2006.
- [28] M. Mehl, B. Uekermann, H. Bijl, D. Blom, B. Gatzhammer, and A. Van Zuijlen, “Parallel coupling numerics for partitioned fluid–structure interaction simulations,” *Computers & Mathematics with Applications*, vol. 71, no. 4, pp. 869–891, 2016.
- [29] E. H. van Brummelen, “Added mass effects of compressible and incompressible flows in fluid-structure interaction,” *Journal of Applied mechanics*, vol. 76, no. 2, 2009.
- [30] U. Küttler and W. A. Wall, “Fixed-point fluid–structure interaction solvers with dynamic relaxation,” *Computational mechanics*, vol. 43, no. 1, pp. 61–72, 2008.
- [31] B. M. Irons and R. C. Tuck, “A version of the aitken accelerator for computer iteration,” *International Journal for Numerical Methods in Engineering*, vol. 1, no. 3, pp. 275–277, 1969.
- [32] B. W. Uekermann, “Partitioned fluid-structure interaction on massively parallel systems,” Ph.D. dissertation, Technische Universität München, 2016.

-
- [33] R. Haelterman, J. Degroote, D. Van Heule, and J. Vierendeels, “The quasi-newton least squares method: a new and fast secant method analyzed for linear systems,” *SIAM Journal on numerical analysis*, vol. 47, no. 3, pp. 2347–2368, 2009.
 - [34] B. Uekermann, H.-J. Bungartz, B. Gatzhammer, and M. Mehl, “A parallel, black-box coupling algorithm for fluid-structure interaction,” in *Proceedings of 5th International Conference on Computational Methods for Coupled Problems in Science and Engineering*, 2013, pp. 1–12.
 - [35] R. Haelterman, A. E. Bogaers, K. Scheufele, B. Uekermann, and M. Mehl, “Improving the performance of the partitioned qn-ils procedure for fluid–structure interaction problems: Filtering,” *Computers & Structures*, vol. 171, pp. 9–17, 2016.
 - [36] D. Blom, F. Lindner, M. Mehl, K. Scheufele, B. Uekermann, and A. van Zuijlen, “A review on fast quasi-newton and accelerated fixed-point iterations for partitioned fluid–structure interaction simulation,” in *Advances in Computational Fluid-Structure Interaction and Flow Simulation*. Springer, 2016, pp. 257–269.
 - [37] F. Lindner, M. Mehl, K. Scheufele, and B. Uekermann, “A comparison of various quasi-newton schemes for partitioned fluid-structure interaction,” in *Proceedings of 6th International Conference on Computational Methods for Coupled Problems in Science and Engineering, Venice*, 2015, pp. 1–12.
 - [38] T. Kajishima and K. Taira, “Immersed boundary methods,” in *Computational Fluid Dynamics*. Springer, 2017, pp. 179–205.
 - [39] R. van Loon, P. D. Anderson, F. N. van de Vosse, and S. J. Sherwin, “Comparison of various fluid–structure interaction methods for deformable bodies,” *Computers & structures*, vol. 85, no. 11-14, pp. 833–843, 2007.
 - [40] C. Degand and C. Farhat, “A three-dimensional torsional spring analogy method for unstructured dynamic meshes,” *Computers & structures*, vol. 80, no. 3-4, pp. 305–316, 2002.
 - [41] A. O. González, A. Vallier, and H. Nilsson, “Mesh motion alternatives in openfoam,” *PhD course in CFD with OpenSource software*, 2009.
 - [42] H.-J. Bungartz, F. Lindner, B. Gatzhammer, M. Mehl, K. Scheufele, A. Shukaev, and B. Uekermann, “precice—a fully parallel library for multi-physics surface coupling,” *Computers & Fluids*, vol. 141, pp. 250–258, 2016.
 - [43] F. Lindner, M. Mehl, and B. Uekermann, “Radial basis function interpolation for black-box multi-physics simulations,” 2017.
 - [44] P. Causin, J.-F. Gerbeau, and F. Nobile, “Added-mass effect in the design of partitioned algorithms for fluid–structure problems,” *Computer methods in applied mechanics and engineering*, vol. 194, no. 42-44, pp. 4506–4527, 2005.
 - [45] C. Förster, W. A. Wall, and E. Ramm, “The artificial added mass effect in sequential staggered fluid-structure interaction algorithms,” in *ECCOMAS CFD 2006: Proceedings of the European Conference on Computational Fluid Dynamics, Egmond aan Zee, The Netherlands, September 5-8, 2006*. Delft University of Technology; European Community on Computational Methods . . . , 2006.

- [46] J. Degroote, P. Bruggeman, R. Haelterman, and J. Vierendeels, “Stability of a coupling technique for partitioned solvers in fsi applications,” *Computers & Structures*, vol. 86, no. 23-24, pp. 2224–2234, 2008.
- [47] B. Uekermann, H.-J. Bungartz, L. Cheung Yau, G. Chourdakis, and A. Rusch, “Official preface adapters for standard open-source solvers,” in *Proceedings of the 7th GACM Colloquium on Computational Mechanics for Young Scientists from Academia*, 2017.